Seasonal Acceleration and Structure of Slow Moving Landslides in the Berkeley Hills

by
Kathryn C. Quigley and Roland Bürgmann[1], C. Giannico and F. Novali[2]

ABSTRACT

Large, slow moving landslides in the Berkeley Hills cause costly damage and pose a potential threat to public safety due to the close proximity of the Hayward Fault. We perform mapping and time-series analysis on InSAR data from two different satellites to investigate the magnitude and seasonal dependence of the landslide motion. Analysis of Interferometric Synthetic Aperture Radar (InSAR) data shows accelerated landslide deformation following periods of increased precipitation, suggesting seasonal dependence. The spatial and temporal coherence of accelerated landslide deformation also increases with higher levels of precipitation. A continuously operating GPS site and borehole inclinometer data in the landslide area show little deformation in the 2007-2008 season consistent with an unusually dry season. Understanding the kinematics of landslide mobility is a first step toward mitigation, in the future we hope to interpret more data from ongoing GPS measurements, ground based LiDAR and new satellite data.

INTRODUCTION

In the Berkeley Hills there are many large, slow moving, deep-seated landslides. This paper focus on four landslides that extend through residential areas and move on the order of cm/year, each covering an area of roughly 0.25-1.00 km^2. Over the years, the landslides have caused costly damage to homes, breakage of underground utility pipes, and confusion over property lines. Although deformation on these landslides is typically quite small and slow, the Hayward fault runs close to (if not through) the head of each landslide (Figure 1). It is currently not well understood how the landslides respond to seismic activity on the Hayward fault, but significant deformation is conceivable under wet conditions and a moderate to large seismic event. We previously inferred that a M=4 event in 1998 below El Cerrito may have advanced a landslide by a few cm (Hilley et al., 2004), but the precision of our measurements did not allow for determining this response in any detail. While there are comprehensive analyses relating triggered landslides on > 20° slopes to the magnitude and nature of strong ground motion (e.g., Meunier et al., 2007), there is little knowledge of the dynamic response of deep-seated slides to shaking. Both scientifically, and for societal reasons, it is very important to understand how deep-seated landslides get mobilized by both precipitation and shaking events, and how such a response scales with the magnitude and duration of such forcing. Even with the current level of ongoing damage there is motivation to mitigate their impact, and the potential hazard to public safety reinforces the need to improve our understanding of these landslides.

In this paper we explore seasonal acceleration of the Berkeley Hills landslides through InSAR data and field research. A previous study by Hilley et al. [2004] used InSAR data from European Remote Sensing satellites (ERS-1 and ERS-2) from 1992-2000 to image the landslides and estimate rates of motion. They suggest that seasonal precipitation levels may accelerate deformation, due to increases in shallow subsurface pore pressure and lithostatic stress gradients. However, they observe a nonlinear relationship between precipitation and deformation, which suggests that near-surface groundwater flow initiates acceleration, but may not further enhance deformation rates beyond a certain threshold level of precipitation.

[1]Department of Earth and Planetary Science University of California Berkeley, Berkeley, CA kquigley@berkeley.edu
[2]Tele-Rilevamento Europa, Milano, Italy

Here we explore InSAR time-series data to gain improved understanding of the seasonal dependence of landslide motion and structural information. We focus on two landslides marked as M and S in Figure 1, representing the Thousand Oaks landslide and the North Berkeley landslide respectively. We utilize an updated processing result of the previously analyzed ERS satellite data (1992-2000) and new data from the RADARSAT-1 satellite between 2001-2006, which has improved temporal resolution and a complementary line-of-sight geometry along which displacements are measured. In addition, there is a local field component to the research involving GPS and borehole inclinometer measurements.

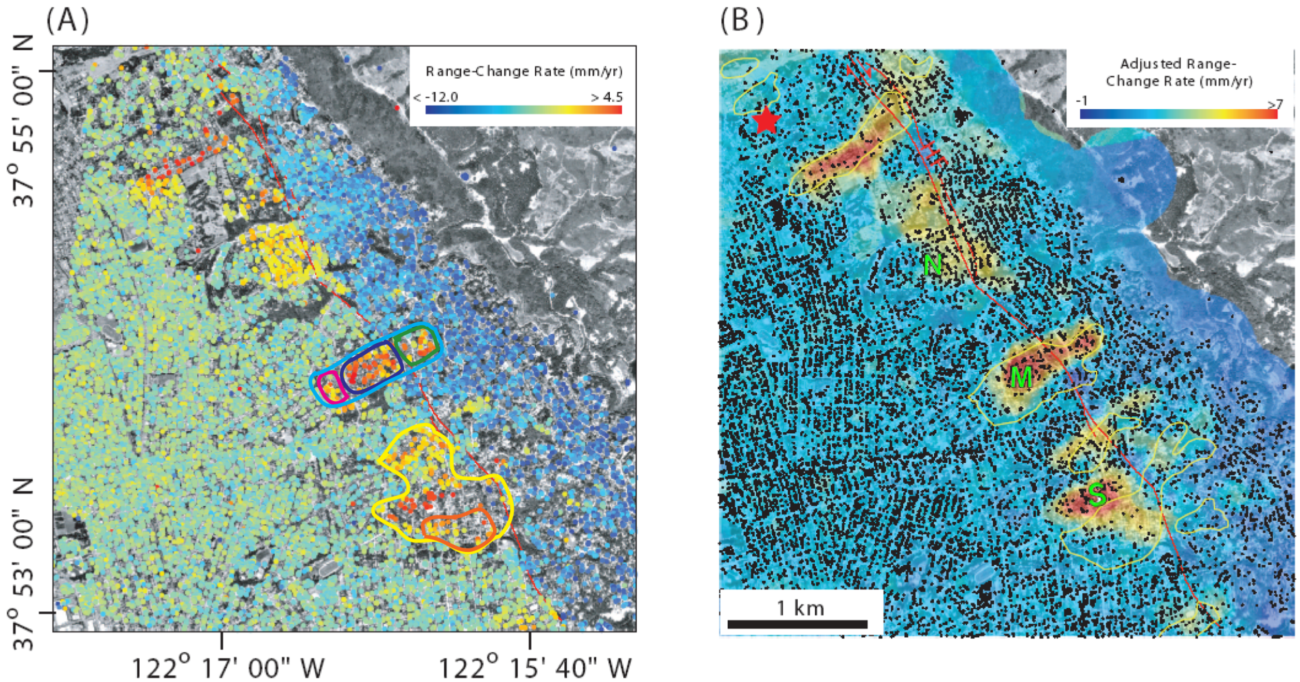

Figure 1. : Each permanent scatterer (PS) pixel in the study area is plotted and colored according to range change rates. The slow-moving landslides of the Berkeley Hills are clearly indicated by the faster moving yellow and red pixels. Positive range change in the ERS data is consistent with southwest motion of the landslides, away from the west-looking satellite. (A) Tectonic surface creep along the Hayward Fault (HF) is clearly visible as a sudden step in range change rate of 1-2 mm/yr. The active trace of the fault from field mapping (Lienkaemper, 1992) is indicated by a red line.Lines drawn around the two south most slides represent 6 groups of coherently moving PS that are used in the time series analysis. (B) Interpolated range-change rates with the range change offset across the Hayward fault removed. The two slides addressed in this study are the Thousand Oaks landslide (M) and North Berkeley landslide (S). The red star shows the location of the M_L=4.1 earthquake (4 December 1998) that appears to have accelerated motion on the nearby landslide (Figure 1 is legible in color on the CD) Modified from Hilley et al. (2004].

InSAR Analysis of Berkeley Hills Landslides

We investigate the structure and seasonal dependence of large, slow-moving landslides in the Berkeley Hills using high-resolution Interferometric Synthetic Aperture Radar (InSAR) permanent scatterer (PS) data from two satellite systems: a pair of European Remote Sensing spacecraft (ERS-1 & 2) and the Canadian RADARSAT-1. Both satellites use radar to measure changes in surface-to-satellite distances (range change); changes in travel time between subsequent passes of the satellite result in radar phase-return shifts and can be displayed as interferograms (e.g., Bürgmann et al., 2000). Permanent scatterers (PS) are typically radar-bright and phase stable structures such as building corners, telephone poles and rock outcrops that can be established in more than ~15 scenes (Ferretti et al., 2000, 2004). Each satellite's data span a greater than five-year time period, during which many passes were made over the study area: between 1992-2000 for ERS and 2001-2006 for RADARSAT-1. For the time series analysis, we do not use ERS data from before 1996, as the temporal sampling is too sparse. For each pixel the PS analysis obtains a time series of relative range change. The ERS data were acquired during descending (towards S13°W) orbits with a west-looking incidence angle of ~23° off-vertical, whereas the RADARSAT data are from an ascending orbit with an east-looking look-angle of 34°. Using Arc Geographic Information Systems (ArcGIS), areas of slow moving deformation are resolved by plotting the PS geographically and coloring them according to their average range change rate (Figure 2).

We use two methods to explore seasonal dependence. The first involves dividing the landslides into groups of coherently moving geographical regions, these groups are each stacked separately. The PS data are combined in groups to improve the signal-to-noise ratio for the detection of seasonal accelerations and to explore the spatial pattern of the deformation. Polygons, drawn on ArcGIS, set the borders of the slide area and regions within the slides that display similar average range change rates. The same polygons are used for both sets of data so that results of the analysis can be directly compared. There are six total groups of PS data defined by polygons. Two of the polygons, Group 1 and Group 5, contain all the points within the Thousand Oaks Landslide and North Berkeley landslide, respectively (Figure 2). For each satellite's dataset the six groups are stacked, detrended, and subsequently plotted as range change by decimal year. Time series of monthly rainfall for the local area are also included on each plot to examine the temporal and spatial relationship between each group's range changes and increased precipitation levels (Figure 3). We find that there is a clear signal showing seasonal dependence in the plots. The coherence of slide deformation between groups increases and the lag time between slide deformation and peak precipitation levels decreases with increasing precipitation levels.

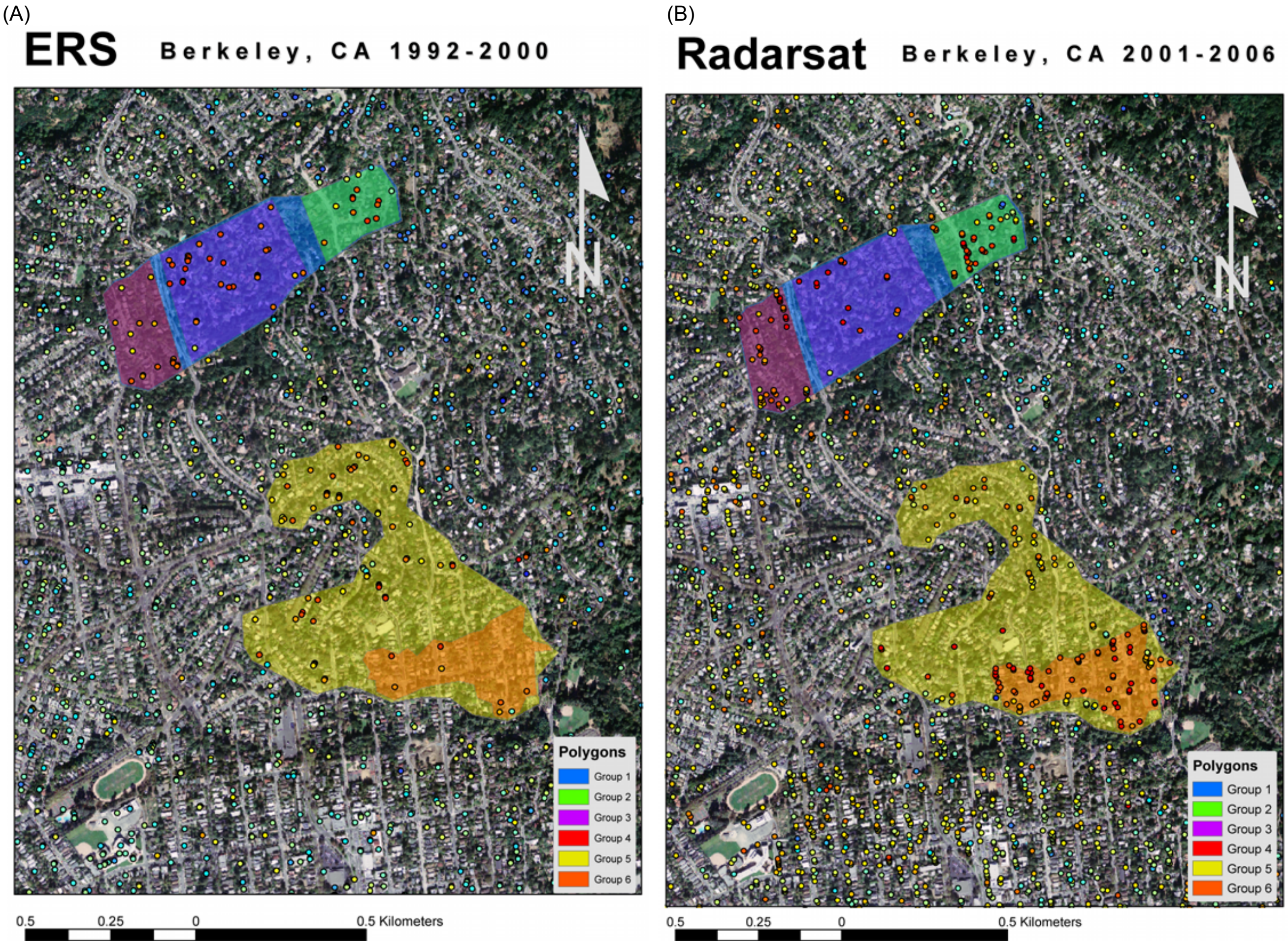

Figure 2. Thousand Oaks and North Berkeley slides and definition of sub-regions selected for time series analysis. Colored polygons represent groups of coherently moving PS for (A) ERS and (B) RADARSAT-1 satellite data. Negative range change in the RADARSAT data and positive range change in the ERS data is consistent with southwest motion of the landslides. (Figure is legible in color on CD.)

The second method involves stacking the data by month, combining the data from all years. Stacking in this fashion also aims to eliminate noise to obtain a clearer pattern of the relative timing of precipitation and slide-velocity peaks. Four plots are generated: one for each combination of satellite and landslide. The range-change time series for the stacked, yearlong periods are detrended and plotted against decimal year. The average rainfall for the local area, which is also integrated by month for the same time span, is also included on each plot to evaluate the temporal relationship between slide motion and seasonal precipitation (Figure 4). We find that there is a clear seasonal dependence and a 0.5-1 month delay between the peak of average slide motion and the peak average rainfall.

The two satellites have different viewing geometries, which allows us to separate contributions from horizontal and vertical slide motions and thus gives the potential to investigate further details of slide deformation and structure through InSAR. The slides move northeast to southwest down the west face of the Berkeley Hills (e.g., Figure 1). The ERS satellites image the slide area from the east and RADARSAT-1 from the west, and thus the southwest moving slides primarily produce positive and negative range-change rates in the ERS and RADARSAT-1 data, respectively. The vertical component of landslide motion (i.e., subsidence) produces range change increase in both data sets. Assuming slide-parallel motion, the average horizontal and vertical rates of the Thousand Oaks slide are 10 mm/yr and 1.5 mm/yr, respectively. Peak rates in the North Berkeley landslide reach 25 mm/yr and 2.5 mm/yr for the horizontal and vertical components, consistent with down-slope motion along the topographic gradient of the slide area (Novali et al., 2005).

(A)

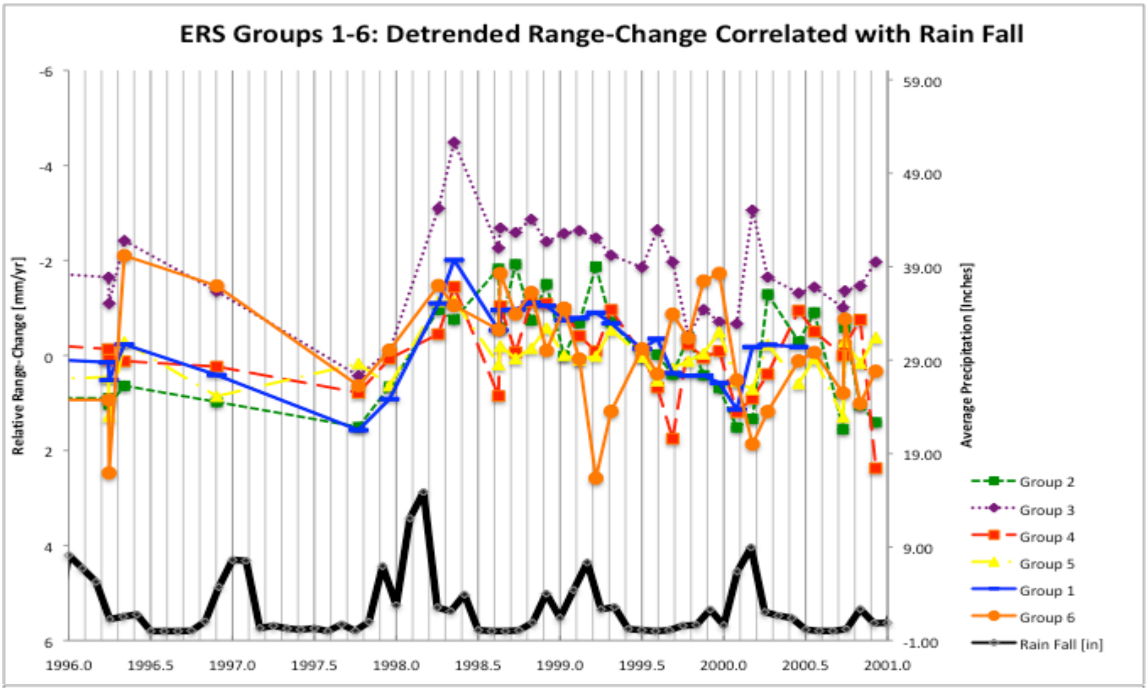

(B)

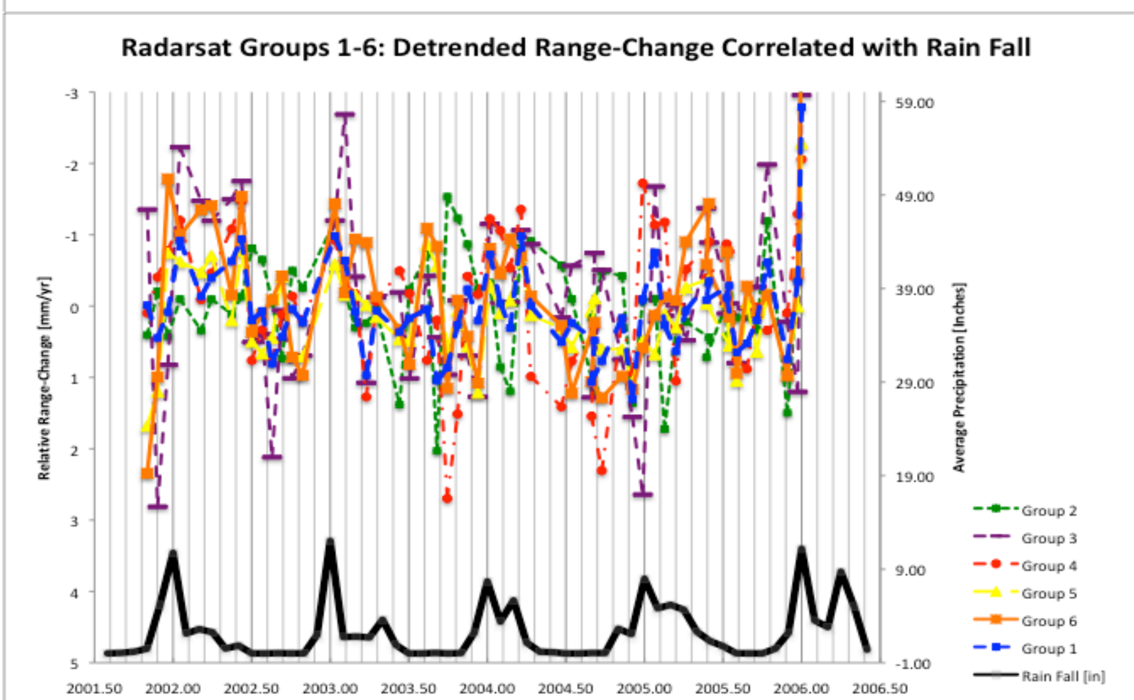

Figure 3. Relative range change of (A) ERS and (B) RADARSAT-1 data (groups 1-6 as mapped in Figures 1& 2) and precipitation as a function of time. Data are detrended and normalized by the average range change, derived from a patch of PS in the non-deforming areas west of the Berkeley Hills. Negative range change in the RADARSAT data and positive range change in the ERS data is consistent with southwest motion of the landslides.

(A)

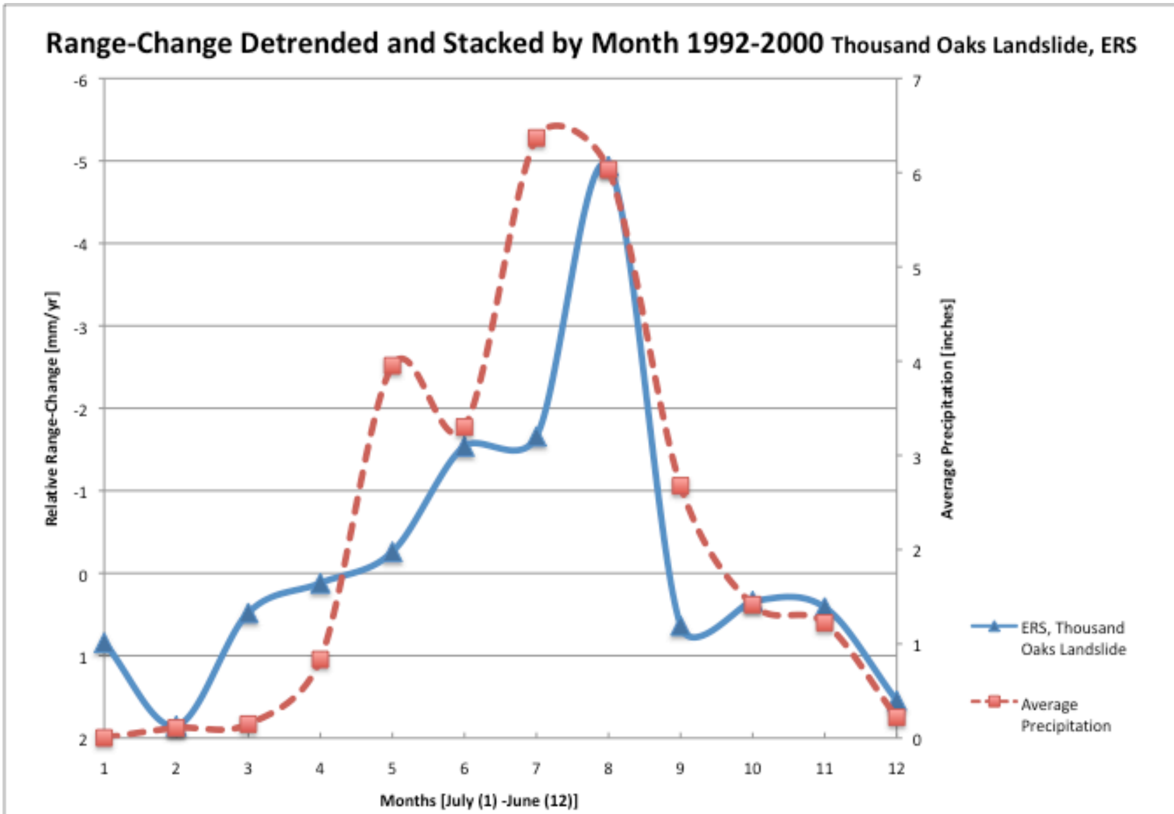
Range-Change Detrended and Stacked by Month 1992-2000 Thousand Oaks Landslide, ERS
Relative Range-Change [mm/yr]
Average Precipitation [inches]
Months [July (1) -June (12)]
ERS, Thousand Oaks Landslide
Average Precipitation

(B)

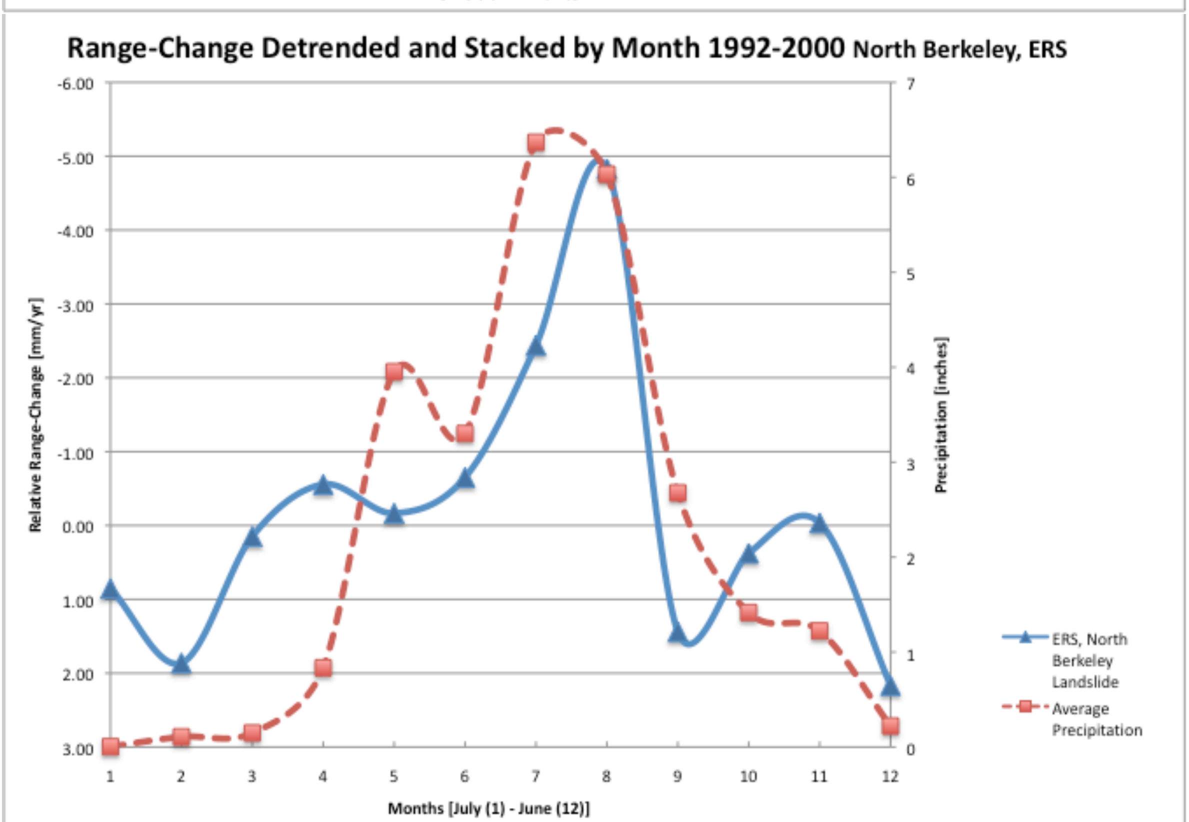
Range-Change Detrended and Stacked by Month 1992-2000 North Berkeley, ERS
Relative Range-Change [mm/yr]
Precipitation [inches]
Months [July (1) - June (12)]
ERS, North Berkeley Landslide
Average Precipitation

(C)

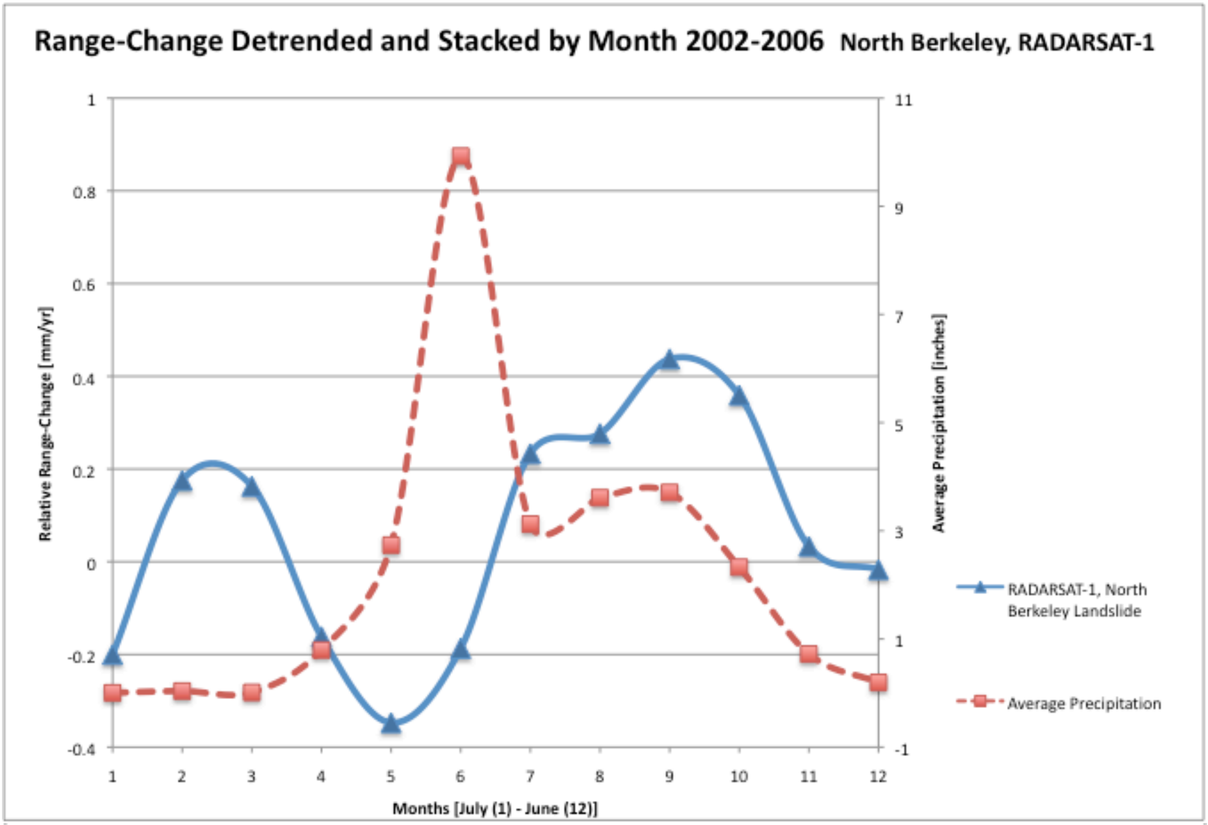

(D)

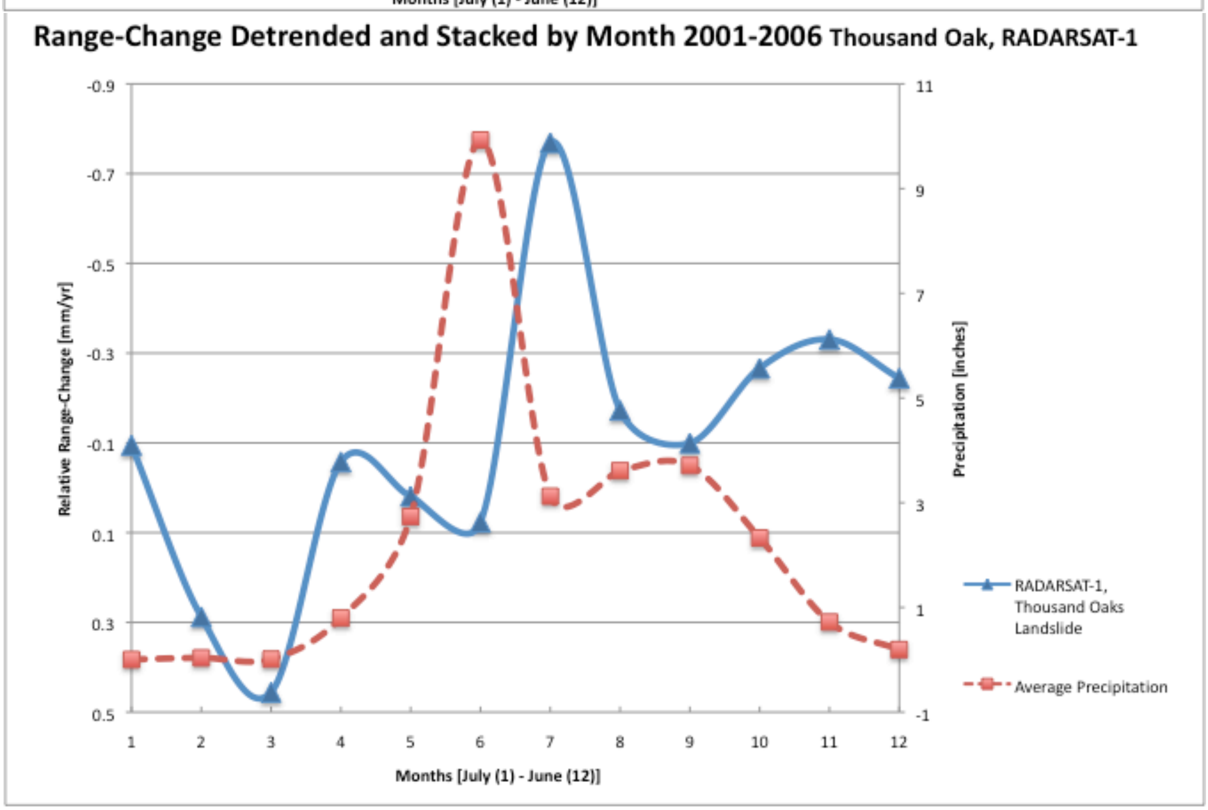

Figure 4. Relative range change of PS are normalized, detrended, and stacked by month for (A) ERS data from North Berkeley, (B) ERS data from Thousand Oaks, (C) RADARSAT-1 data from North Berkeley, (D) RADARSAT-1 data from Thousand Oaks. Each plot includes the average monthly rainfall of the region during the appropriate time series duration for the respective satellite.

While motions along the central portion of a slide should be in the down-slope orientation, rotational motions near the base and head-scarp of the slide help reveal the internal deformation and depth of the slide mass (e.g., Bishop, 1999). Near the head of the slide where landslides generally exhibit localized subsidence, we expect to find an additional component of positive range change in both data sets. At the toe of the slide where sediments pile up we may expect to see uplift and thus somewhat reduced/increased rates in the ERS and RADARSAT-1 data, respectively. Thus, differences in range change at the head and toe of the slide between the two look angles suggest that InSAR has the potential to resolve the internal kinematics of slide motion. A first step towards this process is plotting points selected from a swath about the axis of the Thousand Oaks and the North Berkeley landslides from the ERS-1&2 and RADARSAT-1 data. The PS data along these swaths are then projected onto profiles where the vertical axis is range-change (Figure 5). We find that the RADARSAT-1 data of the North Berkeley slide shows significant sign reversal for points near the head scarp (Figure 5b), suggesting that subsidence there "overpowered" the range decrease from the southwestward motion. There is no clear evidence for strongly rotational motion for the Thousand Oaks slide (Figure 5a), which may suggest that it is not as deep seated. However, more detailed analysis is required to fully resolve the components of surface deformation. In the future, we hope to select collocated points from the two satellites and deconvolve the horizontal from vertical motion from the average velocity. Data from a third viewing geometry are needed to fully resolve the three-dimensional motions of the slides.

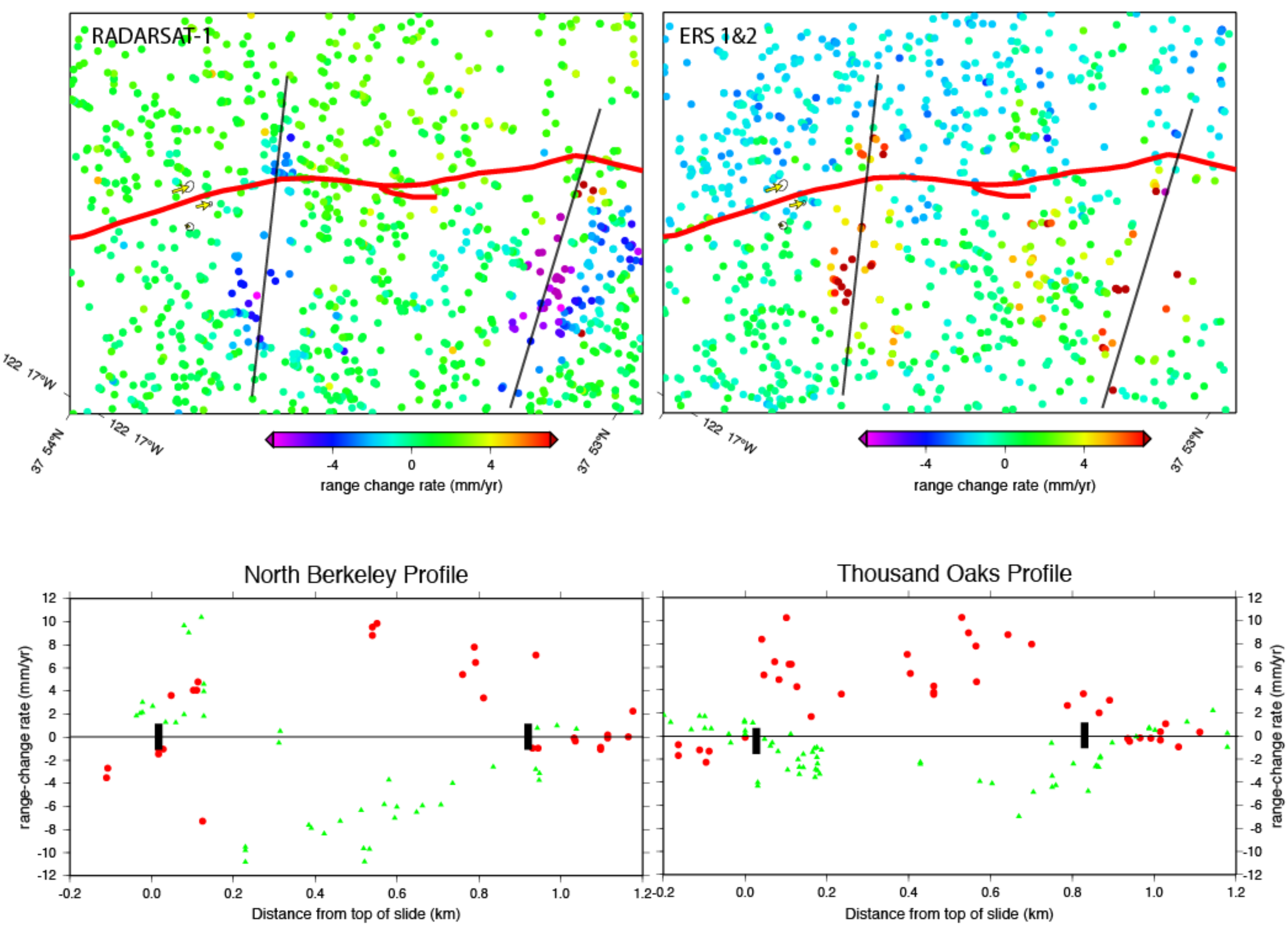

Figure 5. (Top) Maps of range change rate over the Thousand Oaks and North Berkeley landslides. Black dots indicate projected points shown in profiles below. The Thousand Oaks profile is 110 m wide, the North Berkeley profile includes points from a 140-m-wide swath. Negative range change in the RADARSAT data and positive range change in the ERS data is consistent with southwest motion of the landslides. (Below) Down slope profile of range change through both landslides. Red dots and green triangles represent ERS and RADARSAT data, respectively.

DISSCUSSION

The InSAR time series are able to resolve the seasonal acceleration of landslide motion. Research by Hilley et al. (2004) found correlations between InSAR and local rainfall data, which suggest that slide acceleration is modulated by seasonal precipitation. In this study, time-series of landslide motion and average rainfall indicate that the slides are not only seasonally dependent, but are sensitive to variations in the pattern of rainfall between different rainy seasons (e.g., Figure 3). During the strong 1997-1998 El Nino there was a large, narrow spike of rainfall, after which followed a narrow, coherent spike of landslide motion. In contrast the following two rainy seasons were marked by lower levels of somewhat sporadic rainfall, taking place over a wider time period. The time-series for the landslide during this time is marked by similar traits; groups accelerate in a more random, incoherent fashion, which lacks a clear beginning and end to deformation.

Although correlated and highly sensitive, the relation of landslide creep to precipitation levels was found to be nonlinear by Hilley et al. (2004). Precipitation levels in the El Nino year 1997-1998 increased from the typical 0.61 m/year to 6 m/year during a 20-day period of peak rainfall, yet, deformation inferred from InSAR only show an increase from 5.7 mm/year to 11 mm/year. The observed nonlinear relationship between deformation and precipitation indicates that slides may be less sensitive to additional rainfall once they are in motion. Lag times between heavy rainfall and landslide motion observed through InSAR, further suggest that the near surface hydrologic structures may both initiate slide features and buffer slide motion. In the current study, the time-series of geographic groups and average rainfall (Figure 3a,b) show a clear 1-3 month lag for both satellites. The lag is most clearly visible in the years with coherent motion, but is likely present in all seasons and simply masked by the incoherent motion. In the plots that are stacked by month (Figure 4), the lag between the peak of precipitation and the peak in slide motion is especially clear and also ranges from 1-3 months. This result reinforces observations made by Hilley et al. (2004) that deformation tends to occur towards the end of the wet season. Future work could involve analyzing different sub domains of slide areas in greater detail. Additionally, it could also involve exploring the role the Hayward Fault may play in determining where slides are active through the way the HF may affect the distribution of groundwater flow.

Local Field Study at Arch Street 2007-2008 – Preliminary field measurements of slide motion and deformation were carried out on Arch Street, located in the North Berkeley landslide and known to exhibit sizable motion. We installed a continuously operating GPS station setup in a private yard along Arch Street, and two boreholes were established and read by the Alan Kropp Engineering firm (Figure 6). There are also additional ground based LiDAR surveys done before and after the rainy season of 2007-2008, however data is still being processed.

The GPS station consists of an antenna mounted on an eight-foot metal pipe driven four feet into the ground that is connected to a receiver and storage media (Figure 6b). The receiver collected data at a 1 Hz rate during the rainy season of 2007-2008, and continues to collect data at 30-s intervals into the 2008-2009 rainy season. The motivation is to compare the GPS ground motion time series to rainfall and other parameters pertaining to the landslide deformation in the same spatial and temporal extent. Results of the 2007-2008 rainy season show very little deformation (e.g., (Figure 6c)), which may be attributed to the unusually dry season. The borehole inclinometer measures the change in slope of a PVC tube lined borehole. These measurements are taken every several months and can provide estimation for the landslide's depth and rate motion. However, borehole inclinometer readings most likely do not provide the maximum depth of the base of the landslide, given that they are near the edges of the slide region. During the 2007-2008 season, the borehole inclinometer measurements also show very little deformation (0-3 mm/yr) at depth (Figure 6d). We plan to continue the field measurements to provide in situ data on the distribution of landslide motion at the surface and at depth.

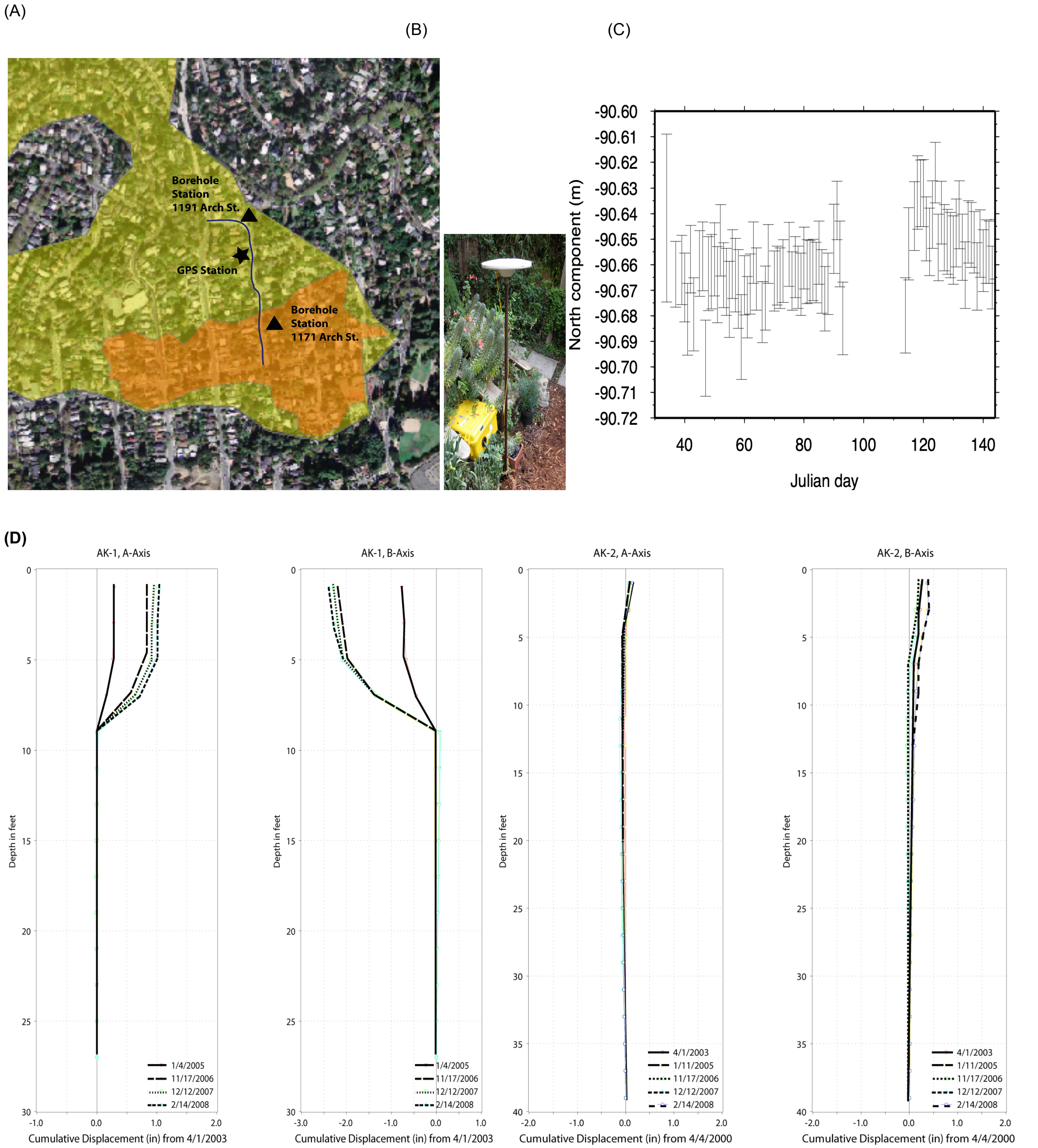

Figure 6. (A) Relationship of GPS and borehole measurements to the location of the North-Berkeley landslide. Arch Street, the position of the GPS receiver and location of the borehole are indicated by the black line and star and triangles, respectively. (B) GPS station set-up being used in North Berkeley landslide study starting in 2007 and still in use. (C) GPS north-component landslide deformation from the North Berkeley landslide station shown in (B) (GPS processing done by Nicolas Houlie, UC Berkeley). (D) Two borehole inclinometer readings indicating the deformation of the landslide as a function of depth. Borehole AK-1 located at 1191 Arch Street (left), and Borehole AK-2 located at 1171 Arch Street (right) (plots courtesy of Alan Kropp).

SUMMARY

This study examined the correlation between seasonal precipitation and landslide deformation. When RADARSAT-1 and ERS data are stacked by month to create a one-year time series, the peak in landslide deformation reveals a lag of 1-3 months relative to the peak in precipitation. The time series for the RADARSAT-1 and ERS data show that movement between areas within each landslide and between landslides became more coherent with increased precipitation. In the future, new data from the GPS station and SAR satellites should further clarify this behavior. During the past 2007-2008 season the GPS data did not record much deformation, which can be explained by the season being particularly dry. The GPS data showed some horizontal but very little vertical motion, which was supported by the borehole inclinometer data.

Acknowledgements

Kathryn Quigley gratefully acknowledges financial support from the Northern California Geologic Society. Project support provided by NASA under award number NNX08AG50G.

REFERENCES

Meunier, P., N. Hovius, and A. J. Haines (2007), Regional patterns of earthquake-triggered landslides and their relation to ground motion: Geophys. Res. Lett., 34, doi:10.1029/2007GL031337.

Bishop, K. M. (1999), Determination of translational landslide slip surface depth using balanced cross sections, Environmental and Engineering Geoscience, 5, 147-156.

Bürgmann, R., Rosen, P.A., and Fielding, E.J., 2000, Synthetic aperture radar interferometry to measure Earth's surface topography and its deformation: Annu. Rev. Earth Planet. Sci., v. 28, p. 169-209.

Ferretti, A., C. Prati, and F. Rocca, Permanent scatterers in SAR interferometry, IEEE Trans. Geosci. Remote Sens., 39 (1), 8-20, 2001.

Ferretti, A., Novali, F., Bürgmann, R., Hilley, G., and Prati, C., 2004, InSAR Permanent Scatterer Analysis Reveals Ups and Downs in the San Francisco Bay Area: Eos, v. 85, p. 317, 324.

Hilley, G.E., R. Bürgmann, A. Ferretti, F. Novali, and F. Rocca (2004), Dynamics of slow-moving landslides from permanent scatterer analysis: Science, 304, 1952-1955.J.D., 1999,

Lienkaemper, J.J., 1992, Map of recently active traces of the Hayward fault, Alameda and Contra Costa Counties, California: U.S. Geol. Surv. Misc. Field Stud. Map, 1:24,000, v. MF-2196, p. 1-13.

Novali, F.; Funning, G. J.; Bürgmann, R.; Ferretti, A.; Giannico, C. (2006) ASF RADARSAT data reveal rates and mechanisms of contemporary surface deformation in the San Francisco Bay Area, Eos Trans. AGU, 87(52), Fall Meet. Suppl., Abstract #H24C-04.

Geographic Information System (GIS) www.ESRI.com